Spatial and temporal risk assessment of Epizootic Hemorrhagic Disease Virus introduction in Europe: A comparative analysis of trade and wind dispersal pathways

Amandine Bibard, Davide Martinetti, Albert Picado, Karine Chalvet-Monfray, Thibaud Porphyre

Preventive Veterinary Medicine 245 (2025) 106656

Contents lists available at ScienceDirect

Preventive Veterinary Medicine

journal homepage: www.elsevier.com/locate/prevetmed

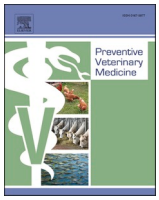

Spatial and temporal risk assessment of Epizootic Hemorrhagic Disease Virus introduction in Europe: A comparative analysis of trade and wind dispersal pathways

Amandine Bibard [a,c,d,*], Davide Martinetti [b], Albert Picado [a], Karine Chalvet-Monfray [c], Thibaud Porphyre [d]

[a] Global Innovation, Boehringer Ingelheim Animal Health France, Saint Priest, France
[b] Biostatistiques et Processus Spatiaux, UR BioSP, INRAE, Avignon, France
[c] Epidémiologie des maladies animales et zoonotiques, UMR EPIA, Université Clermont Auvergne, INRAE, VetAgro Sup, Saint-Genès-Champanelle, France
[d] Laboratoire de Biométrie et Biologie Évolutive, UMR 5558, Université Claude Bernard Lyon 1, CNRS, VetAgro Sup, Villeurbanne, France

ARTICLE INFO

Keywords:
Risk
Culicoides
EHDV
HYSPLIT
Incursion

ABSTRACT

Epizootic Hemorrhagic Disease Virus (EHDV), transmitted by *Culicoides* biting midges, is a threat for the livestock sector in Europe. A quantitative risk assessment model framework was developed to assess the risk of EHDV introduction in Europe, through wind dispersal of *Culicoides* and trade in live animals. The model integrates meteorological data, wind trajectories, vector biology, livestock trade information and considers disease dynamic in infected sources as well as disease susceptibility in potential destinations. The full risk zone combining both pathways encompassed 42 different countries with 30 in Europe and 12 outside, each with highly-variable levels of risk. The highest risk countries included three sources: France, Spain, Italy, and one disease-free, Germany. The period of highest risk corresponded to the favourable period of *Culicoides* activity, between May and October. Risk estimates were markedly higher for the wind pathway, spanning 20 countries mainly in Western Europe, compared to the trade pathway that covered 40 countries, including distant Eastern ones, like Romania. The Pathway Risk Ratio (PRR) showed a higher wind pathway contribution in most countries where both pathways were present. France was the primary source country, regardless of the pathway. Alternative scenarios suggested that limiting the source area to 2024 infected areas or considering long trade history could reduce the list of at-risk countries. However, underreporting or reducing PCR testing at borders could increase risk estimates. This research aims to guide disease risk management measures by providing insights into the risk of *Culicoides*-borne disease extension.

1. Introduction

In Europe, since the 2000s, the livestock sector has experienced frequent waves of epidemics caused by disease virus spread by *Culicoides* spp., including Bluetongue (BTV), Schmallenberg (SBV), and most recently, Epizootic Hemorrhagic Disease (EHDV) viruses. Since 2022, the frequency of these disease introductions has increased. The EHDV serotype 8 (EHDV-8) was first reported in Sardinia and Sicily in late 2022 (Lorusso et al., 2022) and spread throughout the entire Iberian Peninsula within a year, reaching France in September 2023 (Zientara et al., 2024). In addition, Bluetongue serotype 3 (BTV-3) was detected for the first time in the Netherlands in September 2023 (WBVR, 2023), and a new strain of BTV serotype 8 (BTV-8) also appeared in the south-west of France in August 2023 (Gondard et al., 2024). Most recently in October 2024, BTV serotype 12 (BTV-12) was identified in the Netherlands (Loeb, 2024). These hemorrhagic diseases can cause a range of clinical signs in domestic ruminants, which may lead to substantial loss in productivity and, in the most severe cases, to painful symptoms or even death (GDS and ESA, 2024; Santman-Berends et al., 2024). The introduction and spread of these new viral strains are major concerns for farmers and the livestock industry, with potential implications for animal health, animal welfare, and agricultural productivity in Europe.

Among the proposed routes of introduction for such *Culicoides*-borne

* Correspondence to: Boehringer Ingelheim Animal Health France, Saint Priest 69800, France.
E-mail address: amandine.bibard@boehringer-ingelheim.com (A. Bibard).

https://doi.org/10.1016/j.prevetmed.2025.106656
Received 24 February 2025; Received in revised form 30 June 2025; Accepted 8 August 2025
Available online 9 August 2025

diseases, the transboundary trade of live animals has been the focus to date (Gale et al., 2015; Hoar et al., 2004; Napp et al., 2013). Cattle, as the domestic ruminant species the most susceptible to EHDV (Santos et al., 2023), can be infected in one country and then traded for breeding, fattening, or slaughtering to another disease-free area. Undetected infected animals, if transported to areas with suitable conditions for an active vector, can cause subsequent infections at destination. The transport of live animals within the EU accounts for 85% of total livestock trade movements, with the remaining 15% involving trade with countries outside the EU (Massot et al., 2021). Between 2009 and 2015, live animal transport increased by 19% across all species, including a rise in cattle transport from 4.1 to 4.4 million animals. Despite a projected decline fo 9% in beef production by 2035 (EC, 2023) and stringent measures in place in Europe to prevent the transport of unhealthy live animals, the risk of new disease introductions through the cattle trade cannot be ignored. Even though the major cattle trade flows among European countries have been described, changing factors like economy, policies, crises, and market adjustments (Chatellier, 2017) necessitate regular reassessment of trade relations.

Another proposed route of introduction for those vector-borne diseases is the long-distance dispersal of the *Culicoides* midges by the wind. The small size of *Culicoides* spp. makes them susceptible to be uplifted by the wind and dispersed over long-distance, up to 700 km over sea (Ducheyne et al., 2011; Eagles et al., 2014, 2012) and 500 km over land (García-Lastra et al., 2012). For EHDV, this route has been implicated in the first introduction of the viral serotype 2 in British Columbia (Sellers and Maarouf, 1991) and the emergence of viral serotype 8 secondary infections in France (Bibard et al., 2024b). The latter study showed that the EHDV-8 secondary outbreaks followed specific directions depending on the topography and temperature, in correlation with the anisotropic nature of the wind (Bibard et al., 2024b). This underscores the need for wind dispersal simulations in a synoptic approach to predict the extent and direction of potential risk areas for disease introduction.

In this context, Quantitative Risk Assessments (QRA) have been instrumental in estimating disease introduction risks. Recently, QRAs have broadened to include multiple introduction pathways, notably airborne transmission (Simons et al., 2019). However, in this QRA meteorological factors like wind and temperature, which influence virus replication, vector survival, and vector dispersal, were overlooked. In response, we developed a QRA for BTV that integrated atmospheric simulations, specifically adapted to the biological and ecological constraints of the midges (Bibard et al., 2024b). However, our model did not yet consider the commercial trade of animals (Bibard et al., 2024b).

Building on this previous work, our current study aims to provide a comprehensive understanding of the risk of a new EHDV-8 introduction and to inform relevant stakeholders in the field. We sought to identify regions and periods in Europe with the highest risk of EHDV-8 introduction, considering both the trade in live animals between countries and the long-distance dispersal of vectors by the wind, either cumulatively or separately. The goal of our comparative analysis of these two routes of introduction was to identify the spatial and temporal differences in risk predictions and to gain a better understanding of their respective contribution in each country.

2. Material and methods

2.1. Model framework

Fig. 1 provides an illustration of the model framework which encompasses two independent pathways of virus introduction: the wind dispersal of Culicoides vectors and the transboundary trade of live domestic ruminants. This model enhances our previous QRA framework (Bibard et al., 2024a) by incorporating trade pathways and broadening its applicability across Europe. The model can be used at any location within a spatial grid that includes Europe, North Africa, the Balkans, and parts of the Middle East (extending from 28° S to 75° N and 13° W to 40° E) (Supplementary S1.2). This area has been subdivided into grid cells of 0.25° (~25 × 25 km). All cells where at least one EHDV-8 outbreak was reported have been defined as source cells and denoted *i*. The remaining cells of the grid were defined as destination cell and denoted *j*. Following the same logic, any country comprised within the spatial grid was named as a destination country *D* but those counting at least one source cell *i* was named source country *S*. The spatial area encompassing all source cells *i* within a source country *S* has been named, the'source zone' (see description in 3.2). The virus introduction from an infected zone of a source country *S* to any grid cell *j*, involving either infected vectors or hosts, was characterized through successive steps (Fig. 1).

All model parameters are computed by month, with the *m* subscript intentionally omitted in the labels of the variable for the sake of reading clarity.

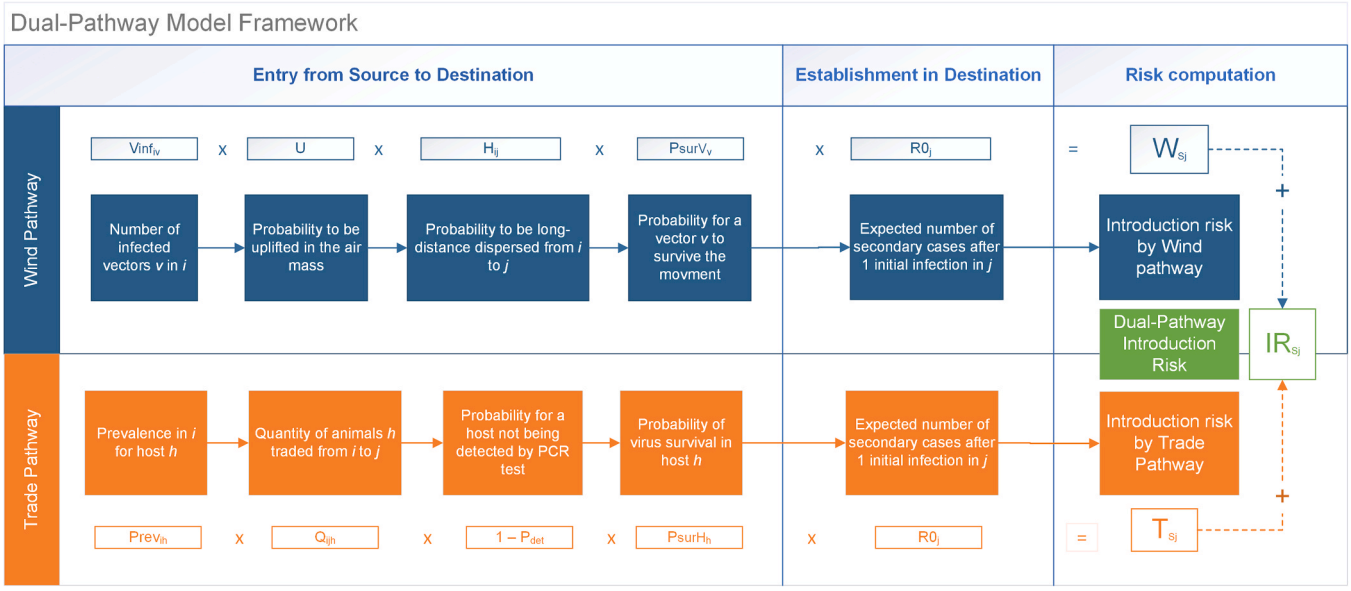

Fig. 1. Overview of the dual-pathway model framework estimating the risk of EHDV-8 introduction in Europe. By each risk pathway and for each source country S, Wind (W_{Sj}) and Trade (T_{Sj}) respectively, are assessed independently through the computations of several steps and finally summed to estimate a dual-pathway Introduction Risk (IR_j) in each grid cell *j* of the spatial grid.

The introduction risk outputs, W_{Sj} or T_{Sj} for the wind of the trade pathways respectively, were calculated for a country source S to any grid cell j, by multiplying each step parameters illustrated in Fig. 1 and further described in Table 1, as:

$$W_{Sj} = R_{0_j} \sum_{i \in S}^{n_i} \sum_{v \in \{1,2\}} V_{\inf iv} \bullet U \bullet H_{ij} \bullet P_{surV_v} \# \quad (1)$$

$$T_{Sj} = R_{0_j} \sum_{i \in S}^{n_i} \sum_{h \in \{c,r\}} Prev_{ih} \bullet Q_{ijh} \bullet (1 - P_{\det}) \bullet P_{surHh} \# \quad (2)$$

With c for 'cattle' and r for 'small ruminants' (the latter representing sheep and goats), the two host species h, and 1 for '*C. imicola*' and 2 for '*C. obsoletus/scoticus*', the two vector species v included in the model.

W_{Sj} was defined as the number of secondary cases that are expected from all grid cells i of country S in a given destination j in a month, knowing the number of *Culicoides* vectors that have been successfully infected ($V_{\inf iv}$), uplifted in the air mass (U), passively dispersed by the wind (H_{ij}), remained live (P_{surV_v}), and further transmit the virus to other individuals (R_{0_j}). The wind dispersal pathway has been inspired from previous risk assessment involving Bluetongue virus, another *Culicoides*-borne disease (Bibard et al., 2024a).

T_{Sj} was defined as the number of secondary cases that are expected from all grid cells i of country S at a given destination j in a month, knowing the probability for a host to be infected ($prev_{ih}$), the quantity of animals to destination j (Q_{ijh}), not being detected by a PCR test ($1 - P_{\det}$), remaining infectious until destination (P_{surH_h}), and further transmit the virus to other individuals (R_{0_j}).

The final monthly risk of introduction in grid cell j, IR_j, was estimated by summing the risk outputs on the two pathways (Fig. 1) and over the n_S source countries contributing to the risk, for a given month as:

$$IR_j = \sum_{S=1}^{n_S} W_{Sj} + T_{Sj} \# \quad (3)$$

The respective monthly risk for wind and the trade pathway in j, were also defined as $W_j = \sum_{S=1}^{n_S} W_{Sj}$ and $T_j = \sum_{S=1}^{n_S} T_{sj}$.

The model was developed in the programming software R version 4.2.2 (Team, 2022). All parameters involved in the model are further described in Table 1.

2.2. Wind pathway

2.2.1. Number of infected vectors in source zone ($V_{\inf_{iv}}$)

In the wind pathway, we first estimated the quantity of infected vectors of each species v in each grid cell i of the source zone included in the source country S for the month m, $V_{\inf_{iv}}$. To do so, we adopted the same approach as in our previous assessment performed for Bluetongue disease (Bibard et al., 2024a). We stated that in each grid cell i a balance equilibrium could be assumed between the different stages - susceptible, latent, and infectious – of the midges and we estimated $V_{\inf_{iv}}$, the number of infected vectors (*i.e.*, the sum of latent and infectious vectors) of species v in each grid cell i according to the number of susceptible vectors $w.V_{iv}$ (abundance) and the monthly prevalence in i, $prev_{ih}$, as follows:

$$V_{\inf_{iv}} = w_i.V_{iv} \quad \frac{1}{\mu_v} \sum_{h \in \{C,SM\}} \beta_v \quad a_v \quad \phi_{vh} prev_{ih} \# \quad (4)$$

where $w.V_{iv}$ is the expected daily number of susceptible vectors of species v in the area i in a given month; μv the mortality rate of vector of species v; βv the probability of transmission from a host species h to a vector of species v given an effective contact; av the biting rate of vector species v; ϕ_{vh} the proportion of vectors species v attracted by hosts species h; and $prev_{ih}$ the monthly host prevalence in i (See details in 2.5). The maximal vector abundance V_{iv} in each grid cell i was retrieved from the VectorNet database (Balenghien et al., 2020) (Table 1).

2.2.2. Long-distance wind dispersal (H_{ij})

To estimate the probability of a midge being dispersed by the wind over a long distance from a specific area to anywhere in Europe, we used a previous methodological approach developed for Bluetongue disease (Bibard et al., 2024a). Briefly, once midges are uplifted in the air mass with the fixed probability U, they are mechanically transported by the wind and reached a destination grid cell j with a probability H_{ij}, estimated such as:

$$H_{ij} = \frac{1}{3} \frac{1}{d_m \alpha} \sum_{y=1}^{3} \sum_{t=1}^{d_m} D_{ijdy} \quad (5)$$

where D_{ijdy} is the number of wind connections between the source cell i and the destination cell j at day d of a given month m and year y; and α is the maximal number of possible destinations reached in a day from a given source cell i, such as $\alpha = 48$ (24 potential deposition spots per trajectory, 2 trajectories started per day). Here, values of D_{ijdy} were extracted from the wind connectivity matrix developed by Bibard et al. (Bibard et al., 2024b), that was specifically developed to identify wind trajectories that can be reached by a given *Culicoides* vector individual within 24 h. Such a wind connectivity matrix was computed over Europe using the atmospheric trajectories simulated by HYbrid Single Particle Lagrangian Integrated Trajectory (HYSPLIT) (Stein et al., 2015) and accounted for the biology of *Culicoides* species in term of midges' flight activity and period (assuming flight activities at sunset and sunrise) as well as their meteorological flight restrictions.

The value of H_{ij} is therefore the mean daily probability of a given destination cell j to be reached by a midge individual departing from a given source cells i, and is averaged over the d_m days of a given month m and across our 3-year study period (2020–2023, excluding 2022 due to an incomplete dataset). Note that atmospheric simulations were not conducted from week 47 to week 10 (~mid-November to mid-March), as this period was not considered part of the *Culicoides* season in most European countries (Versteirt et al., 2017). As such, atmospheric simulations were only performed for the last 15 days of the month of March and the first 15 days of the month of November.

The probability of midge of species v to survive after 24-hour flight for, P_{surV_v}, was also considered (Table 1).

2.3. Trade pathway

2.3.1. Number of traded animals (Q_{ijh})

We collected data between 2015 and 2023 on the monthly number of live ruminants imported into the countries of the study grid, using the online Application Programming Interface of the UN Comtrade database (See Supplementary S1.1 for further details) (UN, 2022) .

As these data inform about animal movements between countries and not at the scale of a grid cell, we extrapolated the number of animals Q_{ijh} of host species h departing from grid cell i located in a given country S to a given grid cell j located in a given country D such as:

$$Q_{ijh} = P_{\exp_i} \bullet Q_{SDh} \bullet P_{arr_j} \# \quad (6)$$

where $P_{\exp_i}$ is the probability of an exported animal originates from cell i of S, whereas P_{arr_j} is the probability of an animal being imported into destination cell j of D. Here, we assumed that these probabilities could be approximated by the proportion of animals present in the country S and the country D, respectively.

We further considered that the monthly quantity of animals of host species h that were traded between S and D, Q_{SDh}, could be approximated by the weight average of the number of animals traded in each month over the 2020–2023 period, such as:

Table 1
List of parameters, notation, description and equations used as inputs in our risk model framework to estimate the risk of EHDV-8 introduction via wind and trade pathways in Europe.

Notation	Description	Value or equation	Reference
n_i	Number of infected grid cells composing the source zone of country S	Grid cell of 25°	-
n	Total number of grid cells in a country S or D	Grid cell of 25°	-
n_S	Number of infected countries S	Depending on scenario considered (4 in baseline)	-
A_{ih}	Number of animal of species h in grid cell i of a country S	Retrieved from Livestock Grid	(Gilbert et al., 2018)
V_{iv}	Maximal vector abundance of species v in grid cell i of a country S	Retrieved from VectorNet	(Balenghien et al., 2020)
N_{Sh}	Total number of EHDV−8 cases notified by the country S over the study period (depending on scenarios) of species h	Retrieved from different epidemiological sources (WAHIS, national databases, French national surveillance platform	
$prev_{Sh}$	Crude host prevalence in the source zone of country S over the study period	$prev_{\mathrm{Sh}} = N_{Sh}/\sum_{i\in S}^{n_i} A_{ih}$	-
w	Probability function of vector presence, such as $w_i.V_i$ is the expected vector abundance of species v in each grid cell i in a given month	$w = \frac{e^z}{1+e^z}$ With z depending on minimal temperature (Φ), minimal relative humidity (ξ) and elevation (Δ) as: $z = -38.964 + 1.166 * \Phi - 0.003 * \Delta + 0.498 * \xi$ Φ and ξ are monthly averages	(Bibard et al., 2024a; Conte et al., 2003)
$prev_{ih}$	Monthly prevalence estimates in grid cell i of country S for species h	$prev_{ih} = w_i.prev_{\mathrm{Sh}}$	-
$V_{inf_{iv}}$	Number of infected vectors in each grid cell i in a given month	$V_{\mathrm{inf}_{iv}} = w_i.V_{iv} \quad \frac{1}{\mu_v}\sum_{h\in\{C,SM\}}\beta_v \quad a_v \quad \phi_{vh} prev_{ih}$	(Bibard et al., 2024a)
a_v	Biting rate of vector species v	$a_1(\theta) = 0.00014 * \theta * (\theta - 3.6966) * (41.8699 - \theta)\hat{}(1/2.7056)$ *for* $\theta > 3.7°C$ (average temperature) $a_2(\theta) = 0.000171 * \theta * (\theta - 3.6966) * (41.8699 - \theta)\hat{}(1/2.7056)$ *for* $\theta > 3.7°C$ (average temperature)	(Aguilar-Vega et al., 2020; Mullens et al., 2004)
β_v	Probability of transmission from a host to vector	$\beta_1(\theta) = 0.0003699\exp(0.1725 * \theta)$ $\beta_2(\theta) = 0.005465\exp(0.159 * \theta)$	(Turner et al., 2013)
μ_v	Natural mortality rate of vector species v	$\mu_1(\theta) = 1 - (1e-5 * \theta\hat{}3 - 0.001 * \theta\hat{}2 + 0.0187 * \theta + 0.8924)$ *for* $\theta > 10°C$ (average temperature) $\mu_2(\theta) = 0.015 * \exp(0.063 * \theta)$ *for* $\theta > 0°C$ (average temperature)	μ_1 (White et al., 2017) μ_2 (Wittmann et al., 2002)
ϕ_{hv}	Proportion of vectors species v attracted to hosts species h	$\phi_{cv} = m_{rv}/(m_{rv} + \sigma_v * m_{cv}) \quad \phi_{rv} = 1 - \phi_{cv} \quad \phi_{h1} = 1 - \phi_{h2}$	-
σ_v	Host preference for vector species v	$\sigma_1 = \sigma_2 = 0.15$ (σ_v<1 indicates a preference for cattle)	(Turner et al., 2013)
m_{vh}	Ratio of vectors species v to hosts species h	$m_{vh} = w.V/A$	-
U	Probability of a midge being uplifted in the air mass	Constant of 0.25	(Bibard et al., 2024a)
P_{surv_v}	Probability of the vector v surviving the movement	$P_{surv} = e^{-\mu_v}$	(More et al., 2017)
H_{ij}	Probability of a vector being dispersed by the wind from the source zone to destination cell j	$H_{ij} = \frac{1}{3\ d_m \alpha}\sum_{y=1}^{3}\sum_{t=1}^{d_m} D_{ijdy}$ with D_{ijdy} is the number of Hysplit connections between the source cell i and the destination cell j at day d of a given month m of year y, extracted from the wind connectivity matrix, α= 48	(Stein et al., 2015),(Bibard et al., 2024a)
Q_{ijh}	Number of animals of species h originating from i of a given country S to a grid cell j	$Q_{ijh} = P_{\mathrm{exp}_i} \times Q_{SDh} \times P_{arr_j}$	-
P_{exp_i}	Probability of an exported animal originates from i of country S	$P_{\mathrm{exp}_i} = A_{ih}/\sum_{i\in S}^{n} A_{ih}$	-
Q_{SDh}	Quantity of animals of species h traded from country source S to destination country D in a given month	$Q_{SDh} = \frac{\sum_y(\omega_y Q_{SDyh})}{\sum_y \omega_y}$ With Q_{SDyh} is the monthly number of animal traded from S to D of year $y \in \{2020, \ldots, 2023\}$ retrieved from UN Comtrade; and ω_y is the weight assigned to year y, such as $\omega_{2023} = 1$, $\omega_{2022} = 1/2$, $\omega_{2021} = 1/3$, $\omega_{2020} = 1/4$	(UN, 2022) Supplementary S1.1
P_{arr_j}	Probability of a host arriving in the grid cell j of the country D from country S	$P_{arr_j} = A_{jh}/\sum_{j\in D}^{n} A_{jh}$	-
P_{surHh}	Probability of a host being still infectious (infectious agent to survive) after the shipment time	$P_{surH_h} = e^{-\left(\frac{t_{shipment}}{t_{lat_h}+t_{\mathrm{inf}_h}}\right)}$ $t_{shipment}$ is the time shipment (in days) between S and D, t_{lat_h} is the latent period before onset of clinical signs in both species (3 days) and t_{inf_h} is viraemia period of host h (30.5 days for cattle and 10 days for small ruminants)	(More et al., 2017) Supplementary S1.2
$1 - P_{det}$	Probability of a host not being detected by PCR testing prior to embarkation	$(1 - \mathrm{P}_{\mathrm{det}}) = 1 - Se_{PCR}$ with Se_{PCR} being the sensitivity of the PCR test for both cattle and small ruminants (0.99)	(AHAW, 2009)
R_{0j}	Basic reproduction Number in grid cell j of country D.	See Supplementary S1.3	(Bibard et al., 2024a; Turner et al., 2013) Supplementary S1.3
δ_h	Recovery rate (1/ duration of viremia in days) in host species h	$\delta_C = 1/29; \delta_r = 1/20$	(Dórea et al., 2017)

(*continued on next page*)

Table 1 (*continued*)

Notation	Description	Value or equation	Reference
d_h	Disease induced mortality in host h	$d_C = 0; d_r = 0.0078$	(Aguilar-Vega et al., 2020; Guis et al., 2012)

Note: ***S*** for a source country, ***D*** for a destination country, ***i*** for source grid cell, ***j*** for a destination grid cell, ***h*** for a host species being either ***c*** for cattle or ***r*** for small ruminants (goats and sheep); ***v*** for a vector species being either 1 for C. *imicola* or 2 for Obsoletus complex

$$Q_{SDh} = \frac{\sum_y (\omega_y Q_{SDyh})}{\sum_y \omega_y} \quad (7)$$

Where Q_{SDyh} is the monthly number of animal traded from S to D of year $y \in \{2020, \ldots, 2023\}$; and ω_y is the weight assigned to year y, such as $\omega_{2023} = 1$, $\omega_{2022} = \frac{1}{2}$, $\omega_{2021} = \frac{1}{3}$, $\omega_{2020} = \frac{1}{4}$. We assumed that weighting each year enhances the relevance of recent data in the average calculation.

2.3.2. Probability of detection (P_{det})

As EHDV is a notifiable disease according to the World Organization for Animal Health (WOAH, 2022) and is listed as category D+E according to the Animal Health Law (European, 2024), commercial trade restrictions are imposed for any animal originating from the infected source zone (excepted for slaughtering). While each destination country has the autonomy to establish its own trade regulations, the Polymerase Chain Reaction (PCR) test is usually mandated to ensure the sanitary status of animals at the border. Therefore we assumed that the probability to be detected at border, P_{det}, can be extrapolated as the sensitivity of the PCR test such as $P_{\text{det}} = Se_{PCR}$,with Se_{PCR} being the sensitivity comprised between 0 and 1, specifically for EHDV (AHAW, 2009).

2.3.3. Probability of virus survival in host (P_{surH_h})

Lastly, as the EHDV infectious state is transient in a host, we considered the parameter P_{surv_h} to estimate the probability for a host to be still infectious once arrived at destination (Table 1). Assuming that this probability depends on the time spent in transportation, we estimated the P_{surH_h}, such as:

$$P_{surH_h} = e^{-(t_{shipment} / (t_{lat_h} + t_{inf_h}))} \# \quad (8)$$

where $t_{shipment}$ is the time (in days) host individuals of species h between source country S and the destination country D, t_{lat_h} is the time period (in days) between the time of infection and that of first clinical signs in host h and t_{inf_h} is time period (in days) of viraemia excretion in blood of host h. In this study, we estimated $t_{shipment}$ using the *google_distance* function of the 'googleway' package (Cooley, 2023), considering traffic conditions, scarcity of road connections and potential sea separation between countries (Further details are provided in Supplementary S1.2).

2.4. Establishment at destination (R_{0_j})

When arriving in a grid cell j, an infected vector or host can be more or less likely to transmit the disease to a local host or vector according to the environmental conditions in j. Similarly to a previous risk assessment performed for Bluetongue (Bibard et al., 2024a), we estimated the potential disease transmissibility of EHDV at destination using the basic reproduction number, R_{0j}, a widely used metric in epidemiology which estimates the average number of secondary cases produced by one infected individual introduced into a population of susceptible individuals (Driessche et al., 2017). Here we used the equation defined specifically for vector-borne diseases by Turner and al. and considering two hosts (Cattle and Small ruminants) and two vectors (*C. imicola* and Obsoletus complex) populations and their interactions and meteorological conditions in grid cell j, primarily the temperature. Because R_0^2 measures the "two-generations like transmission" (Turner et al., 2013), we used the square root, R_0, to estimate the average measure of transmission either from host to vector, like in the trade pathway, or from vector to host, like in the wind pathway. It is also important to note that estimates of R_{0j} were computed in all cell grids showing a vector or a host density of at least 1.6 10^{-4} individual per km^2. See Supplementary Information S1.3 for further details on R_0 equation and parameters.

2.5. Disease information at source

2.5.1. EHDV outbreak locations

We gathered data on all locations where at least one EHDV-8 outbreak has been reported in Europe from 2022 to end July 2024. We preferentially favoured the WAHIS portal as primary data source. However, in cases where the number of infected locations was less than those reported by the EU Animal Diseases Information System (ADIS) (ESA, 2024a), we considered national database when available (Spain) or we manually selected locations based on the map provided by the ESA platform (ESA, 2024a) (Portugal). We finally identified four source zones Z_s in France, Italy, Spain and Portugal, as detailed in Table 2 and illustrated in Fig. 2.

Other source zones were considered depending on the scenario under study, See "Scenarios Analysis".

2.5.2. EHDV prevalence

For each source country S and for each host species h, we first estimated $prev_{Sh}$ a crude country prevalence dividing N_{Sh}, the total number of EHDV-8 cases reported by the country during the study period (ESA, 2024a), by the total number of host individuals A_{Sh} that were recorded present in the n_i grid cells i of the infected zone in S, such as:

$$prev_{Sh} = N_{Sh} / A_{Sh} \# \quad (9)$$

with $A_{sh} = \sum_{i \in S}^{n_i} A_{ih}$, where A_{ih} is the number of host individuals in the grid cell i of the infected zone in S as extracted from the Global Livestock of the World (GLW) database version 4, using population data for 2015 (Gilbert et al., 2018).

To account for the seasonal variations of disease prevalence, due mainly to the *Culicoides* vector activity and then the environmental conditions, we adjusted $prev_{Sh}$ by the probability of *Culicoides* presence w_i that depends on temperature, relative humidity and elevation recorded in each grid cell i (Conte et al., 2003). We further assumed that the prevalence of EHDV-8 in the infected zone in S is homogeneously

Table 2
Characteristics of the Source Zones in the four countries that reported EHDV-8 outbreaks in Europe from 2022 to end July 2024.

Source Country S	Data Source	Period for extraction	Number of Source Cells i included in the Source Zone Z_s
France	WAHIS portal only (WOAH, 2023)	September 2023 – 31st July 2024	55
Italy	WAHIS portal only (WOAH, 2023)	October 2022–2023	2
Spain	Spanish surveillance website (MASA, 2024)	October 2022–31st July 2024	201
Portugal	ESA platform (ESA, 2024a)	2022–31st July 2024	57

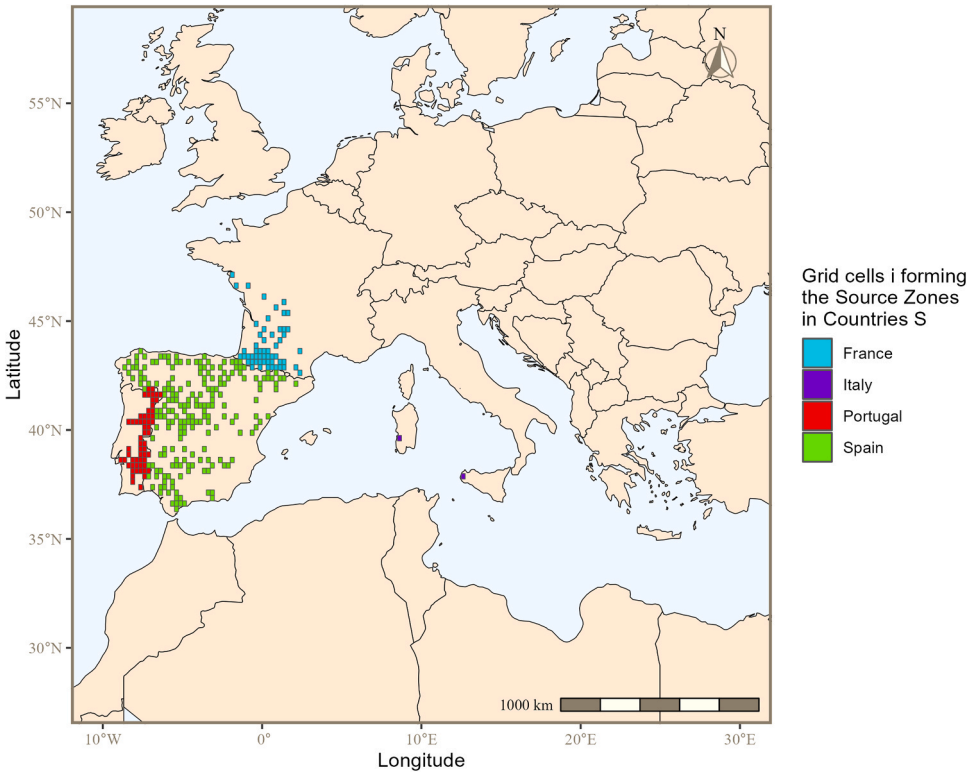

Fig. 2. Definition of the source zones within the source countries S encompassing all the grid cells *i* where at least one EHDV-8 outbreak has been reported between January 2022 and August 2024.

distributed and, thus, estimated the monthly prevalence in grid cell *i*, $prev_{ih}$, such as:

$$prev_{ih} = w_i \bullet prev_{Sh} \# \quad (10)$$

Here, monthly minimal temperature and relative humidity in each grid cell *i* were retrieved from the CHELSA database (Karger et al., 2020), whereas elevation data were retrieved from the European Environment Agency (https://www.eea.europa.eu/).

2.6. Model outputs

For the analysis, the monthly risk outputs at destination *j*, IR_j, were aggregated for each country of destination, IR_D, by summing the risk over the n_j grid cells that compose the destination country, such as $IR_D = \sum_{j \in D}^{n_j} IR_j$, as well as $W_D = \sum_{j \in D}^{n_j} W_j$ and $T_D = \sum_{j \in D}^{n_j} T_j$, for the two independent pathways. Following the same logic, we also computed $W_{SD} = \sum_{j \in D}^{n_j} W_{Sj}$ and $T_{SD} = \sum_{j \in D}^{n_j} T_{Sj}$, being the respective wind and trade risks outputs in country *D* triggered by the source country *S* only. Any cells straddling two countries were excluded from the country-level risk calculation to avoid double counting.

We further computed the yearly average of each risk outputs, i.e. $\overline{T_D}$, $\overline{W_D}$, $\overline{IR_D}$, over the 12-month period (only 8-month period for the wind pathway form March to November), thereby indicating an average number of secondary cases that can be expected in any given month in the destination country *D*. To analyse the respective part of each source country that could contribute to a risk in a country *D* given a specific pathway, we also computed $\overline{W_{SD}}$, $\overline{T_{SD}}$ as the yearly average of W_{SD} and T_{SD}.

Finally, to compare the contribution of each pathways on the total risk of incursion IR_D, a Pathway Risk Ratio (PRR) was computed for each country *D* showing $\overline{W}_D > 0$ and $\overline{T}_D > 0$, such as:

$$PRR = \frac{\overline{W}_D}{\overline{T}_D} \# \quad (11)$$

Here, a value of PRR> 1 indicates that the contribution of the wind pathways in the risk of EHDV-8 incursion is greater than that of the trade pathway, whereas a value of PRR< 1 indicates that such contribution would be smaller.

2.7. Scenario analyses

Six scenario analyses were conducted to evaluate the robustness of

Table 3
Six alternative scenarios tested to evaluate the impact of uncertain parameters on risk outputs. Each scenario is based on variations in biological or methodological assumptions, including trade movements, infectious source zones, under-reporting of outbreaks, and efficiency of surveillance measures.

No.	Biological or methodological assumptions underlying the scenario	Reference
1	Trade movements are not seasonal, and future movements can be inferred from 2015 to 2023 history	-
2	Number and locations of grid cells considered as infectious sources are limited to outbreaks reported in 2024	-
3	Number of reported outbreaks are underestimated by an under-reporting factor of 4 (equivalent to 75 % of under-reporting)	(Simons et al., 2019)
4	Number of reported outbreaks are underestimated by an under-reporting factor of 2.5 (equivalent to 60 % of under-reporting)	(Hartnett et al., 2007)
5	The number of traded animals may not be exhaustively tested by a PCR test; 10 % of them might cross the border without any test	-
6	The number of traded animals may not be exhaustively tested by a PCR test; only half of the animals might be tested	-

the risk outputs to variations in assumptions regarding trade movements, initial source zones, and efficiency of surveillance measures (Table 3).

In Scenario 1, we assumed that there is no seasonal pattern of the trade imports between countries, meaning that each monthly movements of animals are independent from each other. In this case, the monthly quantity Q_{SDh} of animals traded from country S to country D was inferred over the history of the monthly trade movements since 2015, estimating for each month, host species h, and pair $S-D$. To do so, we considered $Q_{SDh} = Q'_{SDh}$, where Q'_{SDh} is the simulated number of animals moving between S and D such as:

$$Q'_{SDh} = L_{SDh} \bullet M_{SDh} \# \quad (12)$$

where $L_{SDh} \sim Bin(l_{SDh})$ and $M_{SDh} \sim Pois(m_{SDh})$, with l_{SDh} and m_{SDh} are the probability of trade movement occurring and the expected number of animals moving between S and D, respectively. Here, we estimated the value of l_{SDh} by dividing the number of month where at least one animal of host species h moved between S and D over the total number of months in the study period during which a trade event could have occurred. In contrast, the expected number of animals moving between S and D, m_{SDh}, was computed as the mean number of animals of host species h that were traded monthly between S and D.

In Scenario 2, we restricted infected grid cells considered in our analysis to those where EHDV-8 outbreaks were reported in 2024 only (between June and end of August). This assumes that grid cells where outbreaks occurred in 2023 are not infectious anymore due to a sufficient level of herd immunity. Estimates of $prev_{Sh}$ were therefore adjusted accordingly. For France, the locations of EHDV-8 outbreak in this scenario were manually selected based on the map provided by the national surveillance platform (www.platforme-esa.fr).

In scenarios 3 and 4, we considered that the reporting of EHDV-8 cases by a country could not be exhaustive and might be underestimated for several reasons, including the lack of exhaustive testing on farms. This is particularly plausible in the situation where farms were either previously found infected or located within an infected area and showing animals with suggestive clinical signs. We multiplied the observed number of reported outbreaks N_{Sh} by an under-reporting factor, χ, either $\chi = 4$ (Scenario 3) or $\chi = 2.5$ (Scenario 4), thereby increasing the estimate of EHDV-8 prevalence $prev_{Sh}$.

In scenarios 5 and 6, we hypothesized that PCR tests may not have been carried out exhaustively prior exportation movement. As such, the probability of non-detection $(1 - P_{det})$ can be modified such as:

$$(1 - P_{det}) = P_{no-test} + (1 - P_{no-test}) \times (1 - Se_{PCR}) \# \quad (13)$$

where the parameter $P_{no-test}$ denotes the proportion of animals that were not tested by PCR. Here we considered either $P_{no-test} = 0.1$ (Scenario 5) or $P_{no-test} = 0.5$ (Scenario 6).

3. Results

3.1. Risk hotspots

3.1.1. At country level

The total risk zone encompassing countries with $\overline{IR_D} > 0$ was broadly distributed over 42 countries, including 30 European and 12 non-European countries (Fig. 3). The total surface of this zone covers 541

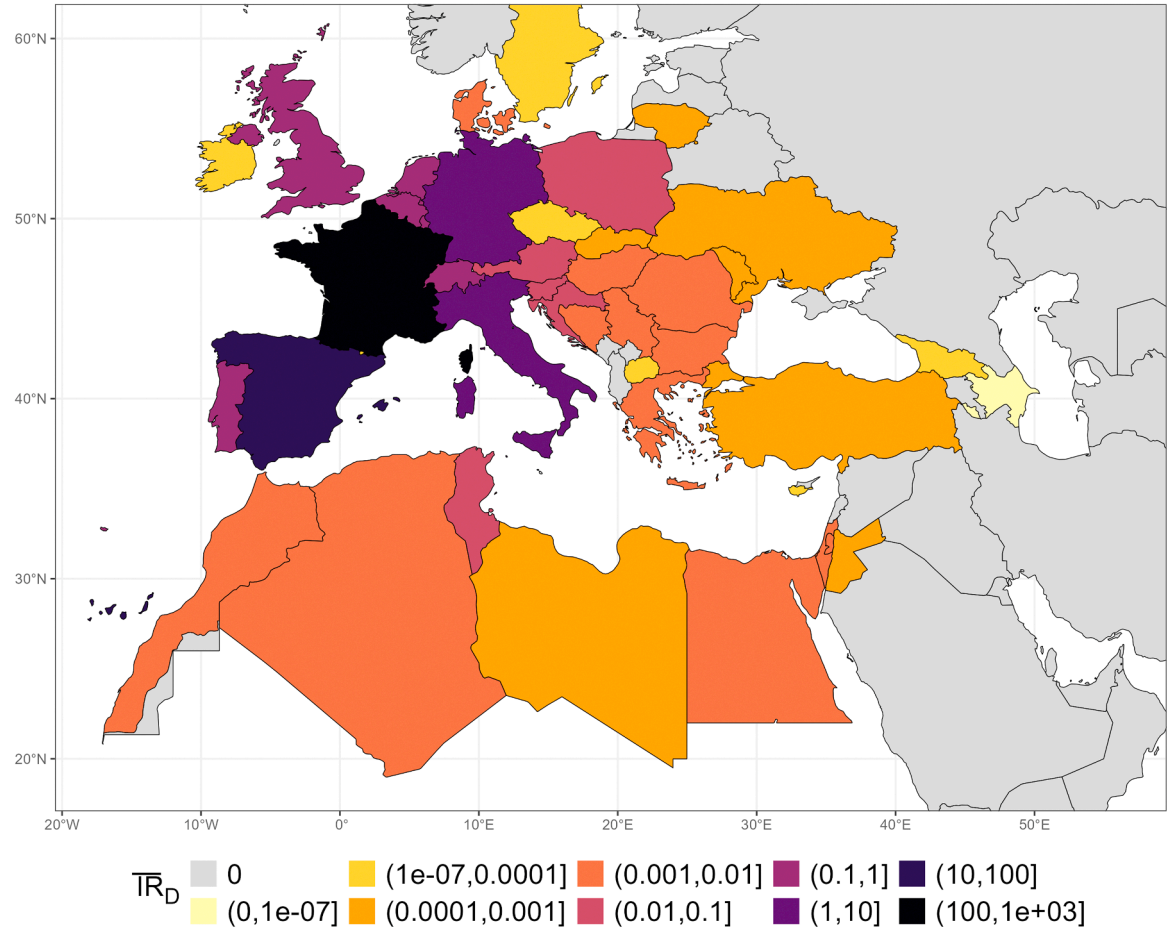

Fig. 3. Spatial distribution of $\overline{IR_D}$, the mean monthly risk of EHDV-8 introduction per destination country D. The risk output considers here both the wind and the trade pathway cumulatively.

million hectares. However, the level of risk per country was highly variable ranging from ~8.7 10^{-10} to 747 potential secondary infections per month in average (Fig. 3). The countries that showed higher risk estimates were France, Spain, Italy and Germany ($\overline{IR_D} \in [1;747]$), followed by Belgium, Switzerland, Portugal, United Kingdom, Luxembourg and Netherlands ($\overline{IR_D} \in [0.1;1]$) (Fig. 3). Despite their geographical proximity to Spain and Portugal, it's interesting to note that Morocco and Algeria displayed risk levels comparable to those observed in distant countries, such as Denmark and Romania. As expected, the Eastern countries and the northernmost country, Sweden, exhibited the lowest risk category (Fig. 3).

3.1.2. At grid cell level

At the grid cell scale, the risk map of $\overline{IR_j}$ highlights the most at-risk regions within each country. Fig. 4 depicts results for France, Italy, Germany and United Kingdom and the results for other countries are presented in Supplementary Information S2.1.

In France, the grid cells with the highest risk categories ($\overline{IR_j} \in [1;50]$) were in the southwestern region from the Atlantic border to the western edge of the Mediterranean Basin. Considering $\overline{IR_j}$ of [0.1;1], the grid cells at-risk covered a substantial part of central mainland France. Interestingly, the grid cells in the south-east of France had no risk or the lowest category.

In Italy, grid cells with the highest risk category, ranging between 1 and 10, were exclusively located in Sardinia and Sicily. However, some with lower risk grid cells were also found in the central region, with sporadic occurrences in the southern part of the Italian peninsula.

For Germany, only the western regions of the country showed few cells with $\overline{IR_j} > 0.01$, namely Saarland, Rhineland-Palatinate, and the south-western parts of North Rhine-Westphalia and Baden-Württemberg. In the United Kingdom, only the eastern part of the country was dotted with grid cells of the lowest risk categories $\overline{IR_j} < 0.01$.

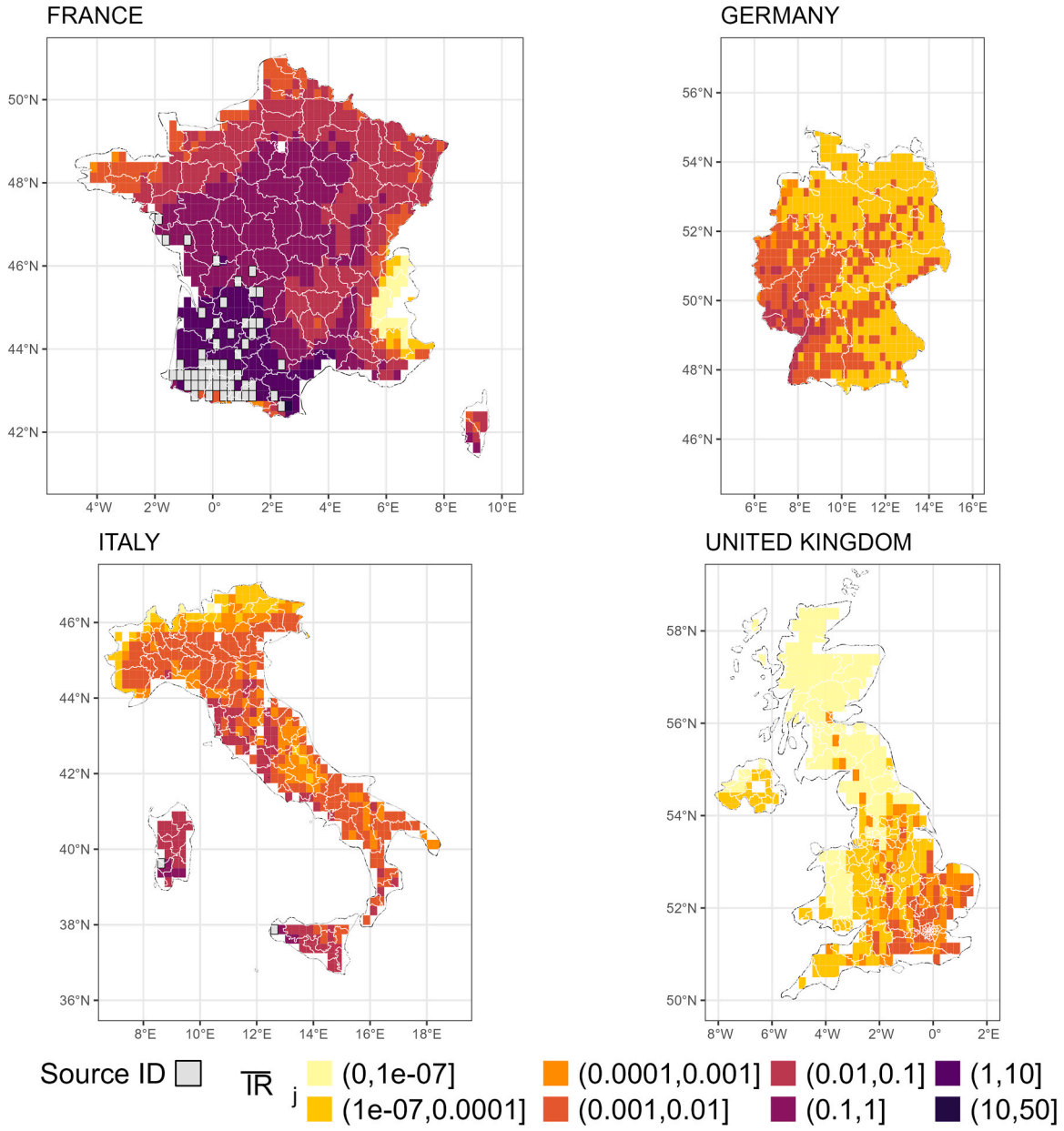

Fig. 4. Spatial distribution of $\overline{IR_j}$, the mean monthly risk of EHDV-8 introduction per grid cell, and specifically depicted for France, Italy, Germany and United Kingdom. In both France and Italy (Sardinia and Sicily), the infected source grid cells are represented by the grey grid cells encircled by a black colour. The risk output considers here both the wind and the trade pathway cumulatively.

3.2. High-risk periods

Fig. 5 represents the temporal variation per month of the country monthly risk when considering both trade and wind pathways, and expressed in log scale, $\log(IR_D)$. The spatial distribution of IR_D is presented in Supplementary S2.3, while the boxplots of $\log(W_D)$ and $\log(T_D)$ for each pathway are shown in Supplementary S2.4.

The median of log IR_D across at-risk countries increased from January to May, was roughly stable from June to August, and decreased from September to December (Fig. 5). During the winter and cooler months from December to February, when the risk due to the wind pathway was null, the trade pathway contributed to a very low but minimal risk in about ten countries, mostly located in southern Europe or North Africa (See Supplementary S2.3 & S2.4).

3.3. Comparison between pathways

3.3.1. At country level

Fig. 6 depicts separately the level of risk per country due to the Wind, $\overline{W_D}$ and due to the Trade, $\overline{T_D}$.

In considering solely the wind pathway (A), the total risk surface ($\overline{W_D} > 0$) encompasses 176 million hectares, covering 20 countries, with 16 in Europe and 4 outside (Tunisia, Algeria, Morocco, and Libya). The countries with the highest $\overline{W_D} \in]10; 10^{+3}]$, were indeed some source countries, such as France, Spain, and Italy. Interestingly, Germany, a country free from the disease and neighbouring the source countries, exhibited a risk category equivalent to Italy. The lowest risk category ($\overline{W_D} < 10^{-3}$) was observed in countries far distant from the source countries, such as Ireland, Croatia and Libya.

Regarding the trade pathway (B), the total surface of risk ($\overline{T_D} > 0$), covers 529 million hectares, covering 40 countries, with 30 in Europe and 10 outside. Countries with the highest level of risk were those with $\overline{T_D} \in]10^{-1};1]$, such as Italy and Spain. Croatia and Slovenia shared the second highest risk category with $\overline{T_D} \in]10^{-2}; 10^{-1}]$.

3.3.2. Pathway contribution

As illustrated in Fig. 7, the risk ratio of wind over the trade pathway (PRR) is presented for each country. In countries where both pathways contribute to the risk, the PRR was predominantly greater than 1, highlighting the significantly higher contribution of the wind pathway, as compared to the trade pathway. This is observed for most of the European countries, and with a more pronounced effect (>1000 times higher) in France, Austria, Germany and United Kingdom. The exceptions are Croatia, Greece, and Ireland where PRR< 1, due to a $\overline{T_D}$ being within the moderate to high-risk category of the pathway, unlike $\overline{W_D}$. Most of the Eastern countries of Europe showed no PRR meaning that the risk was exclusively due to trade pathway. Conversely, in Algeria and Libya, the risk was triggered exclusively by the wind pathway.

3.3.3. Source country contribution

Fig. 8 represents a heatmap of risk highlighting the contribution of each source country *S* to the risk in a destination country *D*, regarding either the wind pathway (*A*) or the trade pathway (B) independently.

Regardless of the pathway, France was the primary source country contributing to a large proportion of risk across a wide range of destination countries, including itself. France is also the unique source that contributes to a risk by the wind in Germany, Switzerland, Luxembourg and for the most part to Belgium, United Kingdom and Netherlands. Conversely, Portugal presented a minimal risk contribution to a limited number of countries, particularly when considering the wind pathway. Interestingly, Portugal contributed to a risk in distant countries by the trade pathway, such as Israel and Palestine. Italy contributed to a trade risk in a broad range of destination countries, but its contribution to wind risk was restricted to a limited number of countries. Spain significantly contributed to the risk in France and Portugal, primarily through the wind pathway, and was also responsible for risk in Eastern European countries such as Croatia and Slovenia by trade pathway.

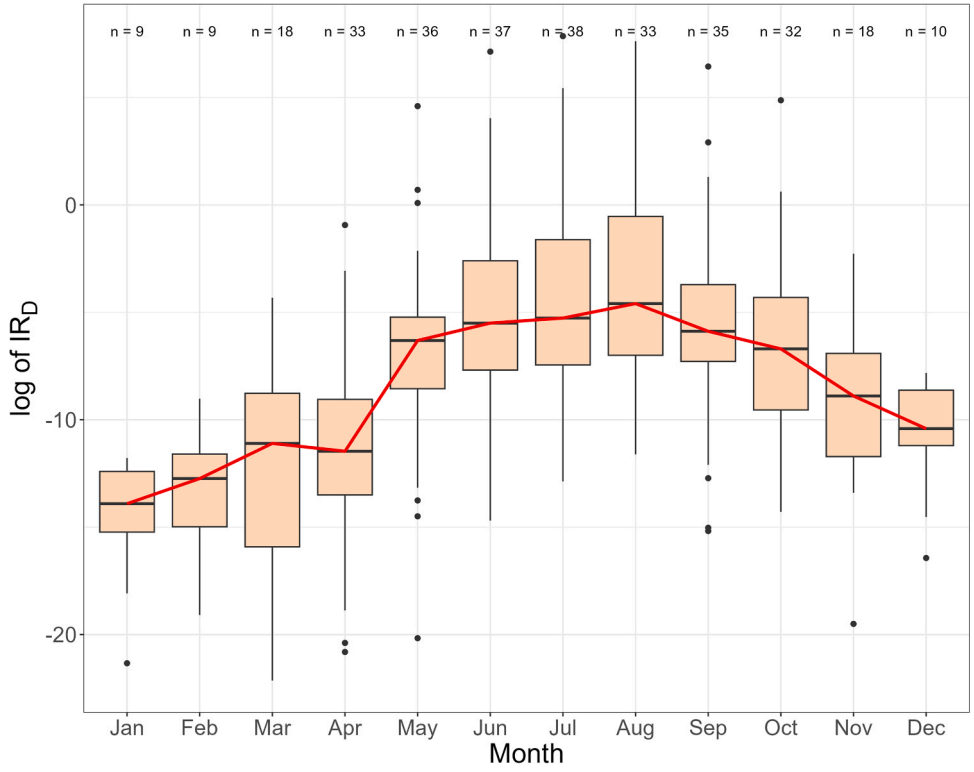

Fig. 5. Temporal variation of monthly risk estimates in countries, IR_D, in log scale. Here IR_D considers the contribution of both pathways of introduction. The red line joins the median values of the distributions. The number n above each month represents the number of destination countries considered in each distribution ($IR_D > 0$).

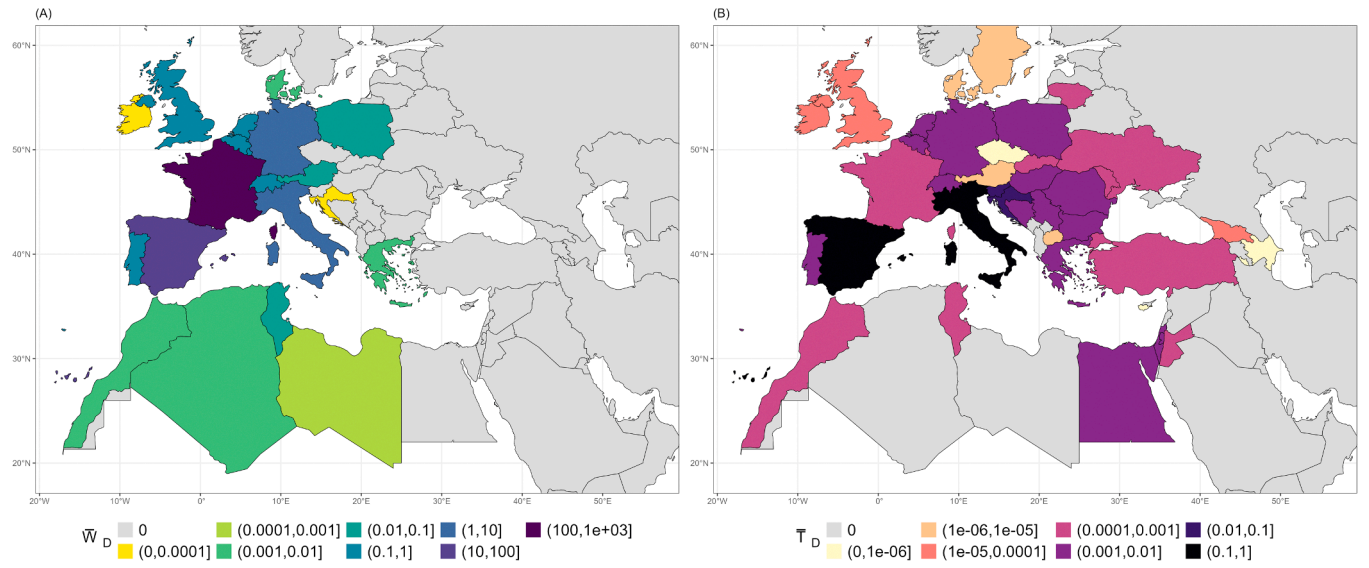

Fig. 6. Spatial distribution of $\overline{W_D}$ (A) and $\overline{T_D}$ (B), the respective Wind and Trade mean monthly risk per destination country D.

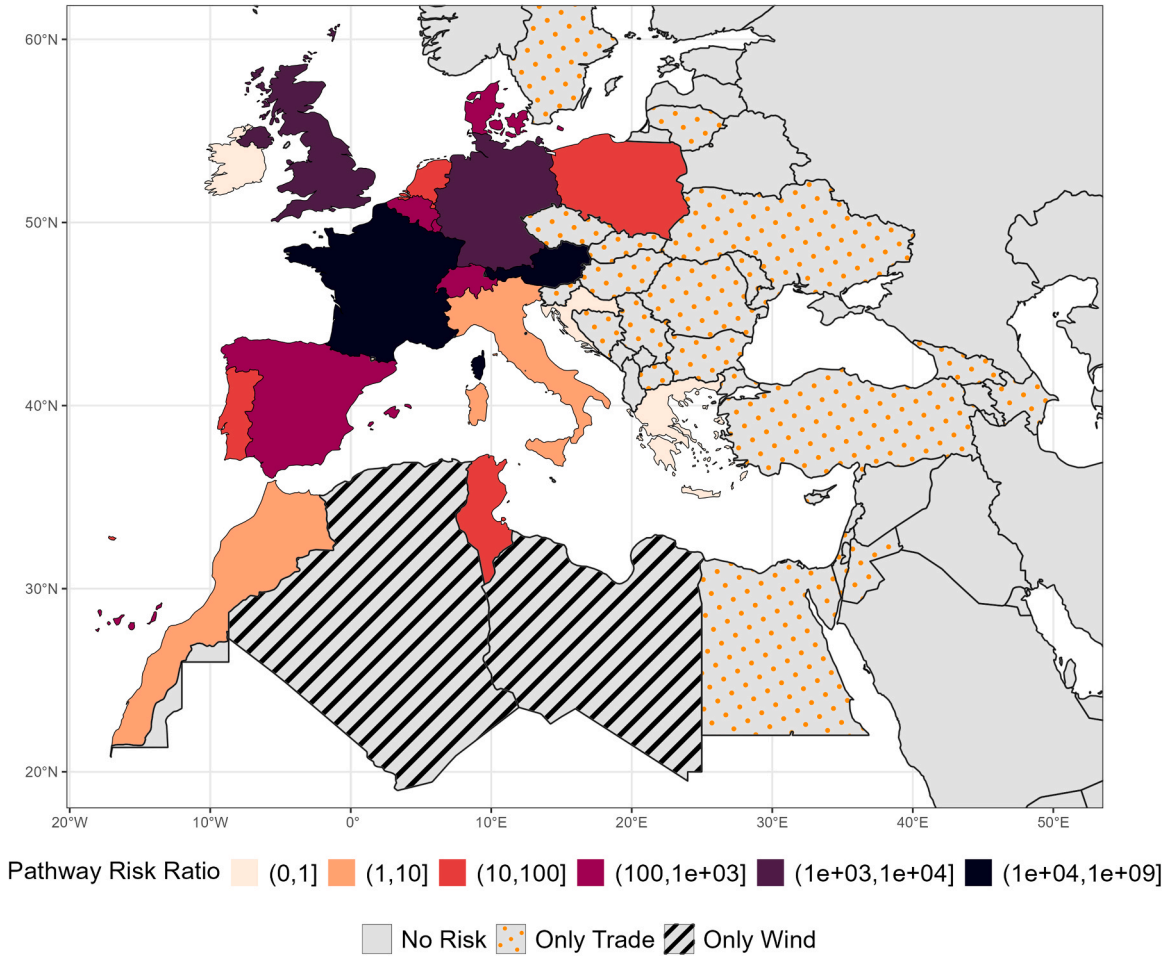

Fig. 7. Pathway Risk Ratio (PRR) per destination country. Colours indicate countries where both pathways contribute to the risk; patterns indicate countries where only one pathway contributes. PRR is the ratio of the Wind over the Trade mean monthly risk (PRR = $\overline{W_D}/\overline{T_D}$).

3.4. Impact of scenarios

We assessed the impact of uncertainty by considering different scenarios. The distributions of each of the risk outputs, $\overline{IR_D}$, $\overline{W_D}$, $\overline{T_D}$ in log scale for each scenario are shown in Fig. 9, considering either the two pathways cumulatively (A) or wind (B) and trade (C) separately. The source zones considered in scenario 2 are presented in Supplementary S2.5. The impact of all scenarios on the spatial distribution of $\overline{IR_D}$ is

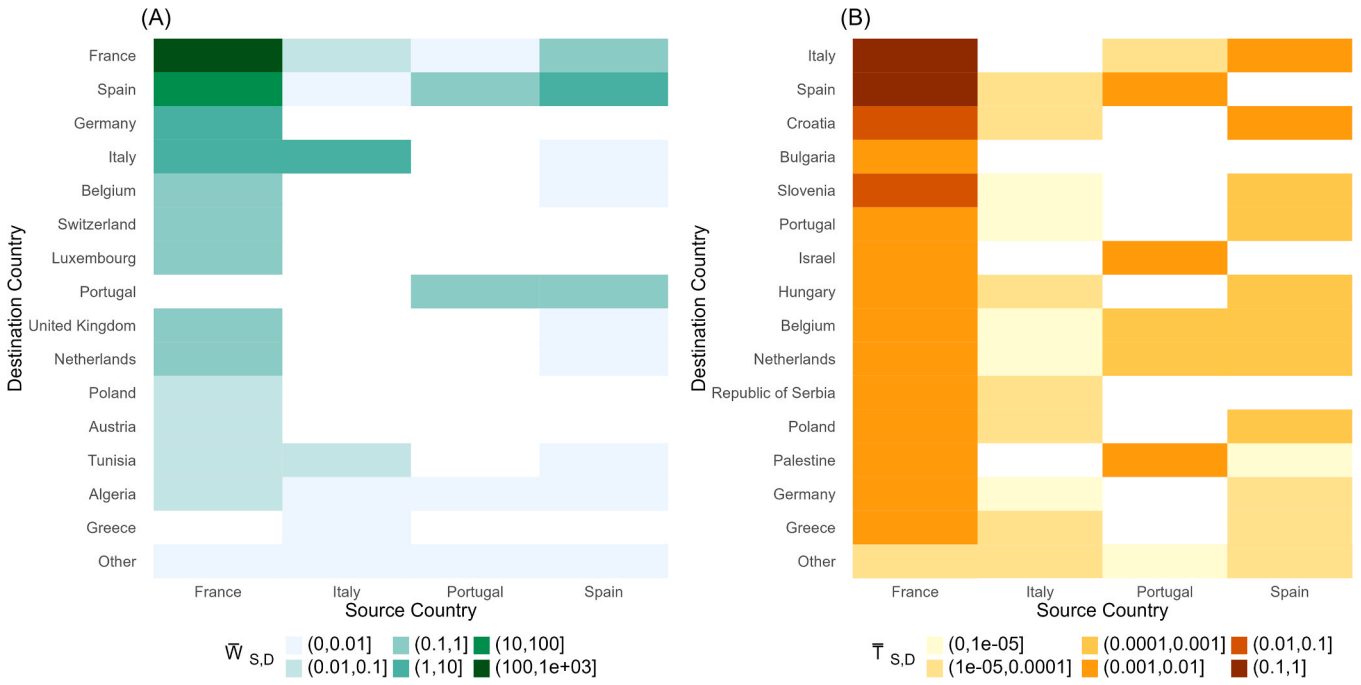

Fig. 8. Heat maps showing (A) $\overline{W_{S,D}}$ and (B) $\overline{T_{S,D}}$, the monthly risk estimates between each combination of source S and destination D countries, considering independently and respectively the Wind Pathway or the Trade Pathway. For the sake of clarity, only the 15 destination countries with the highest $\overline{W_{S,D}}$ and $\overline{T_{S,D}}$ were depicted and the others summed under "Other" category.

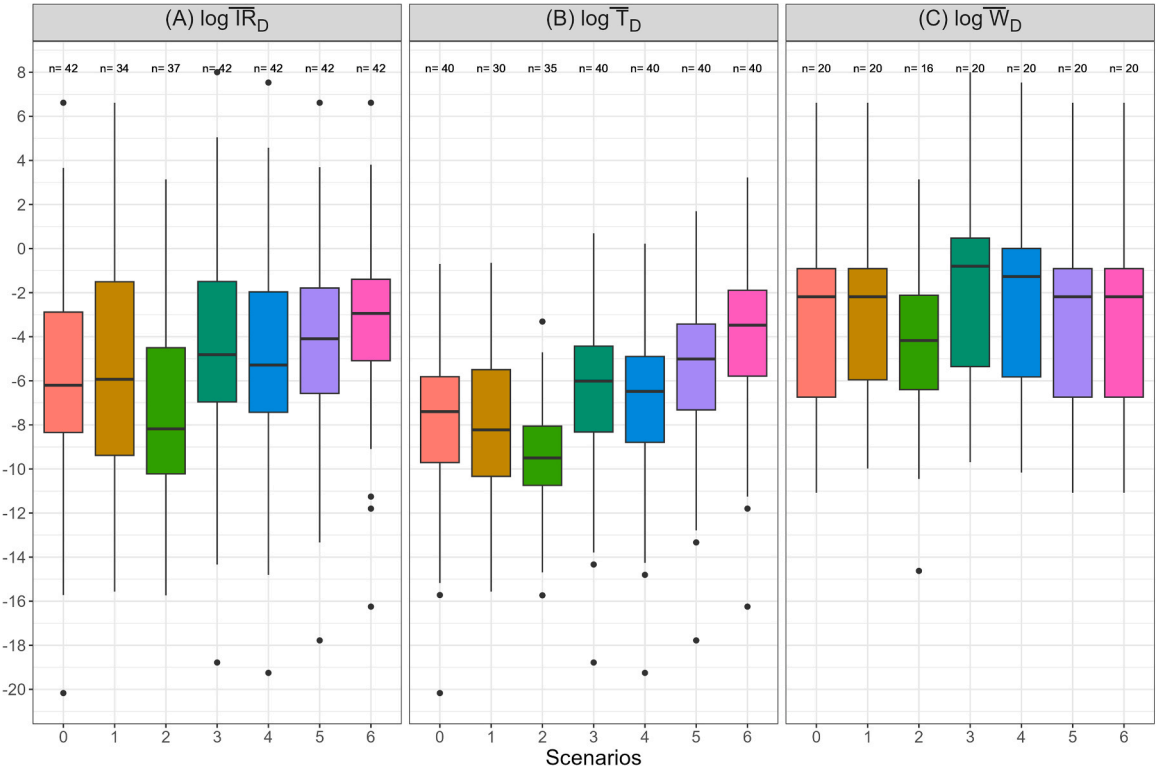

Fig. 9. Impact of different scenarios on the distributions of mean monthly risks per destination country $\overline{IR_D}$, $\overline{W_D}$, $\overline{T_D}$ in log scale, considering either the two pathways of introduction cumulatively (A), or only the wind (B) or only the trade pathway alone (C). The number n at the top of each distribution represents the number of countries that are included in each distribution. The definition of each scenario is presented in Table 2.

detailed in Supplementary S2.6.

Compared to the baseline, the scenario 1 that inferred trade movements from a longer historical period, led to a decreased median of risk $\overline{IR_D}$ by $+0.27$ log (*i.e.,* 1.48 times higher) across the countries but reduced the number of countries at risk from 42 to 34 (Fig. 9), with 9 less countries and 1 additional one (Russia) (Supplementary S2.6). As expected, the effect was only observed on the trade risk outputs. While the median log of $\overline{T_D}$ has decreased in scenario 1, the trade rank of the

countries changed and have increased the risk for some countries with already a high $\overline{W_D}$ risk, as Italy, Spain and France.

In comparison to the baseline scenario, scenario 2 considered the EHDV outbreaks occurring only in 2024 and in this case, the results showed a marked reduction in the median of log $\overline{IR_D}$ by −1.9 log (*i.e.,* 10^{-2} times), illustrating a decrease for most of the countries (Fig. 9). For instance, the $\overline{IR_D}$ for France was 23.1 instead of 747 in baseline. The number of countries at-risk also decreased to 37 countries (Fig. 9), with Austria, Libya, Sweden, Cyprus, Azerbaijan not being at-risk anymore (Supplementary S2.6). Both trade and wind risk outputs showed a reduction mostly because the EHDV-8 prevalence within the source zones of countries *S* were reduced, except for Portugal (data not shown). The spatial covering of the source zones in Spain and Portugal was also more restricted (northern regions) and only slightly more extended in France (Supplementary S2.5). Italy was no longer considered a source country, while Andorra was.

With the scenarios 4 and 3, that assumed increasing level of under-reporting of the EHDV cases (60 % and 75 % respectively), the median of log $\overline{W_D}$, $\overline{T_D}$, and then $\overline{IR_D}$ increased proportionally as compared to baseline (Fig. 9), due to a higher level of infection in the source countries. However, the spatial at-risk zone in destination countries was unchanged (Supplementary S2.6). France, the highest risk country, would have a $\overline{IR_D}$ of 1867 and 2988 considering respectively 60 % and 75 % of under-reporting, as compared to 747 in baseline.

Finally, when considering 10 % (scenario 5) or 50 % (scenario 6) of non-tested animals at the border, the median of $\overline{T_D}$ was increased respectively by 128 times (+2.1 log) and 1801 times (+3.25 log) (Fig. 9), with no change in the spatial zone predicted at risk (Supplementary S2.6).

4. Discussion

In this study, we identified European regions and time periods of heightened vulnerability of EHDV-8 incursions based on 2022–2024 situation.

Our results demonstrated that the spatial distribution and the level of the EHDV-8 risk were dependent on the nature of the introduction pathway considered. The wind dispersal pathway was identified as the primary contributor to the overall risk level, aligning with our expectations given that wind-borne transmission is a major route for the spread of *Culicoides*-borne diseases. Considering this pathway, the hotspot countries were the source countries (France, Spain, Portugal, Italy), as well as disease-free neighbouring countries such as Germany. This is consistent with the most favourable conditions for 24-h *Culicoides* flight aided by wind currents. Our risk maps, analysed at the grid cell level, underscored the presence of significant wind patterns within each country. For instance, in the Iberic peninsula, the major winds appeared to predominantly move from South to North / Northeast, as it was previously observed during the Bluetongue serotype 1 (BTV-1) epizootic coming from Morocco (Diego et al., 2014). From the southwest region of France, a major wind current seems to go from South to North along the western coast, avoiding the Massif Central Mountain. This southwestern part of France was previously infected by BTV-1 coming from Spain, but the disease did not spread northwards thanks a massive and mandatory vaccination campaign at the time (Kundlacz et al., 2019). Furthermore, our predictions indicated that central France exhibited a higher level of risk compared to the west coast (Brittany and Normandy) (Fig. 4), two key cattle farming regions—central France predominantly focused on beef production and Brittany on dairy farming. In scenarios where vaccine availability would be limited, prioritizing vaccination in the highest-risk areas would be recommended. While our model currently does not account for differences in farming management systems when estimating exposure through R_0, this could be addressed in future model refinements. Our results highlighted wind corridors at risk that are important to consider for efficient management and control of *Culicoides*-borne diseases.

In contrast to the wind pathway, the contribution of the trade pathway to the overall risk level was estimated as low. This could be attributed to the stringent preventive measures in place of trans-boundary animal trade or the relatively low number of animals exported from the source countries each month. We further showed that incomplete animal testing by PCR test (10 % or 50 %, Scenarios 5 & 6) would significantly increase the final introduction risk level. Nevertheless, the trade pathway maintains a baseline level of risk during cooler periods when wind-borne transmission is unlikely and extends the risk to more distant countries. Italy and Spain were the two highest countries at risk by the trade pathway, in accordance with their respective rank #1 and #3 as importer of cattle in Europe (Rossi, 2020). Interestingly, the Netherlands, which is at the rank #2 of the cattle importers in EU (Rossi, 2020), showed a lower risk in our model. This is mostly because the animals imported to Netherlands usually do not come from the three main infected countries (France, Spain, Portugal) but from others like Germany and Belgium. It is therefore likely that risk of EHDV-8 introduction into the Netherlands would drastically increase if either of these latter countries were to become infected.

Additionally, our results showed highest risks during the months from May to October, which corresponds to the usual period of EHDV-8 outbreaks reporting for most of the European countries (WOAH, 2023). This timeframe also aligns with the most favourable season for Obsoletus complex activity (predominant midge species), forecasted between week 25 and week 52 over most of the European countries (Versteirt et al., 2017). However, it should be noted that no wind simulations were carried out in Hysplit during the winter period from 15 November to 15 March, based on the assumption that low temperatures would preclude virus replication in the vector (Carpenter et al., 2011). Therefore, wind dispersal during this period made little or no contribution to the overall risk by methodological design. However, this assumption could be challenged in light of the reported occurrences of BTV-3 outbreaks during the winter months of 2023/2024 in northern European countries (ESA, 2024b) and the observed increase in global surface warming since 1990 (Samset et al., 2023).

Using our model, we additionally highlighted the important contribution of France to the future risk of EHDV-8 introduction in Europe, irrespective of the pathway considered. This can be explained by its central geographical position within Europe, which places France at the crossroads of various wind and trade pathways. Furthermore, France holds the leading position as a cattle exporter in Europe, particularly to Italy with the weanling's market (Rossi, 2020). Therefore, our results underscored the necessity to foster resources and prevention activities in this country to efficiently limit or block the global spread of EHDV-8 across Europe. In this context, the vaccination program already initiated by France (MASA, 2024) may be beneficial for the whole of Europe.

Our model has its limitations. In particular, the accuracy of our risk estimates relies heavily on the quality and completeness of the input data, including reported EHDV-8 cases and locations, meteorological conditions, and trade data.

On one hand, the prevalence of EHDV-8 outbreaks, as calculated within each infected country, may potentially be underestimated despite our efforts to consolidate outbreak information from diverse data sources. The countries usually provide exhaustive reports of case numbers and locations to the World Organization for Animal Health (WOAH) during the early stages of an epidemic. However, as the situation becomes endemic, these reports may transition to a less detailed, quarterly consolidated format, lacking in precise geographic or chronological information. It can be then reasonably assumed that the true estimate of risk might be closer to those incorporating under-reporting (scenarios 3 & 4). However, in this case, the hotspot countries would remain unaffected. On the other hand, changing the geographical extension of the source zone, as focusing on the most recent 2024 outbreaks (scenario 2), had significantly changed both the hotspots' countries and the level of risk. In this scenario 2, we observed a

significant reduction in the number of at-risk countries and in the risk level of each country, due to a reduced prevalence and a more restricted source zone (excepted in France) compared to the baseline results. It emphasizes that our model's accuracy depends on a precise definition of the source zone, both spatially and quantitatively, to closely match the ongoing epidemiological situation at the time of the risk assessment. It must be acknowledged that the potential for vaccination programs in source countries was not considered in the current model, which might result in a conservative estimate of prevalence within certain regions.

While our model provides a forward-looking perspective on the risk of EHDV-8 introduction, it is important to note that the meteorological data used in our model are based on historical values, which may not accurately predict future weather conditions. Therefore, a high uncertainty remains around the extension of wind trajectories and disease transmission parameters which both depend on temperatures. An interesting further development of our model could be to integrate future climate scenario data into the Hysplit model to prospectively explore the impact of exceptionally warm years, such as what was experienced in 2023 globally (WMO, 2024). From a methodological standpoint, although the use of wind trajectories simulated by Hysplit has demonstrated its ability to accurately predict the location of secondary outbreaks (Bibard et al., 2024b), it has also been shown to underestimate the number of new cases occurring within the source grid cells, *i.e.,* any location within a 25 km radius around the centroid of source cell. For this reason, we can also assume that the risk estimated for the wind pathway solely, might be underestimated in the destination countries that are also a source country. It might be particularly true in the case of small countries like Andorra in Scenario 2 (composed if only 1 grid cell), or when a significant proportion of the country grid cells are infected source cells (Portugal and Spain in baseline scenario).

To account for the movement of live animals between countries in our risk assessment framework, we used the extensive and open access database of the United Nations 'UN Comtrade'. The quality and completeness of the data largely are contingent on the reporting countries, which can vary significantly. Despite the data curation efforts by the database administrators, there might be instances where some country data is incomplete, incorrectly attributed to a wrong month, or published late. To mitigate the latter bias, we excluded data from 2024 from our risk assessment. Nevertheless, our analysis based on long-term historical exchanges (scenario 1), identified Russia as a potential destination country, which may not be relevant considering the current trade and political relationships with Europe. This situation underscores the need for a balanced approach, using recent but not too recent data, to accurately capture the dynamics of bilateral trade agreement. A key issue with trade data is the lack of fine-scale information on final destinations of animals within destination countries. We then assumed that the traded animals were distributed proportionally to the host density. While it might seem reasonable to assume that areas with high animal density could be the most probable destinations, the risk dilution across grid cells makes it challenging to identify high-risk zones. Furthermore, the European legal framework concerning Animal Welfare may impose stricter regulations and controls on long-trip journeys, in line with the Farm to Fork European strategy (Molitorisová and Burke, 2023). These regulations were not considered in our current study. Lastly, our risk assessment framework did not consider the illegal animal movements as another potential risk pathway.

Our deterministic framework was parametrized from literature or existing databases such as livestock density, vector abundance, wind connectivity matrix, and trade data. This data-driven approach, while robust, does not provide a clear understanding of the uncertainty surrounding each parameter and, cumulatively, on the final risk estimates. We opted for a scenario-based approach, which allowed us to evaluate separately the impact of changes in trade, surveillance, and epidemiological situations. However, many other parameters, particularly those related to EHDV-8 transmission remained unknown or poorly quantified. For instance, the vector competence, which has been evidenced as a significant parameter in the introduction risk for BTV-3 (Bibard et al., 2024a), was not specific to EHDV-8 in *C. imicola* and the Obsoletus complex but derived from literature for BTV in *C. sonorensis*. Therefore, we could suggest to further improve the model adopting a probabilistic approach (parameter described by a probability distribution), which could better quantify the concomitant impact of all parameters on the final risk outputs. We could also advocate for new vector competence studies in *Culicoides* spp. even regarding EHDV serotypes that not yet been introduced in Europe.

Regarding the potential establishment of the disease at destination, we decided to use the R_0 metric which considers two vector species and two host species (Turner et al., 2013). Although apparently complex, this equation would allow R_0 not to be underestimated in areas where two vector species coexist and can lead to cross-infections in hosts, such as in the southern parts of Europe (Santman-Berends et al., 2013). However, in most of the European countries, the R_0 in our study was mainly driven by Obsoletus complex, with higher values in areas where the ratio of Obsoletus complex abundance to host abundance was higher (Supplementary S1.3). The contribution of small ruminants was very limited compared to cattle (data not shown). Finally, in this case study we obtained a spatial distribution of R_0 per month globally similar than the one calculated per week in the case of BTV-3 model in accordance with previous literature (Bibard et al., 2024b). It should also be noted that EHDV-8 may be transmitted by other *Culicoides* species than the two included in this framework.

5. Conclusion

In conclusion, our dual-pathway model highlighted a wide but heterogeneous risk zone of EHDV-8 introduction across 42 countries, with Southwestern Europe identified as significant hotspots. The wind dispersal has been identified as the primary risk pathway in most of countries while the trade of animals contributed to low but basal risk in distant countries and during cool periods. France was a key source country by both pathways. These results contributed to an efficient management of EHDV-8 in Europe.

CRediT authorship contribution statement

Amandine Bibard: Writing – review & editing, Writing – original draft, Visualization, Software, Methodology, Funding acquisition, Conceptualization. **Thibaud Porphyre:** Writing – review & editing, Funding acquisition, Conceptualization. **Karine Chalvet-Monfray:** Writing – review & editing, Conceptualization. **Davide Martinetti:** Data curation, Conceptualization. **Albert Picado:** Writing – review & editing, Conceptualization.

Declaration of Competing Interest

Amandine Bibard is an employee of Boehringer Ingelheim Animal Health in France and has received a research grant to complete her Ph.D. from the French Government through the "Plan de Relance" initiative (ANR-21-PRR-0075–01). Albert Picado is an employee of Boehringer Ingelheim Animal Health. Thibaud Porphyre is financially supported by the French National Research Agency and Boehringer Ingelheim Animal Health France through the IDEXLYON project (ANR-16-IDEX-0005) and the Industrial Chair in Veterinary Public Health. HYSPLIT data were produced by Davide Martinetti within a mutual agreement between VetAgro-Sup and INRAE. Karine Chalvet-Monfray declares no commercial or financial relationships that could be construed as a potential conflict of interest.

Acknowledgements

AB gratefully acknowledge the support received from the French Government through the "Plan de Relance" initiative (ANR-21-PRR-

0075–01). TP would like to thank the French National Research Agency and Boehringer Ingelheim Animal Health France for support through the IDEXLYON project (ANR-16-IDEX-0005) and the Industrial Chair in Veterinary Public Health, as part of the VPH Hub in Lyon.

Supplementary Material

Supplement S1 provides additional information regarding the material and the methods, such as Comtrade data collection (S1.1), the road time calculation between countries (S1.2), the R_0 calculation (S1.3). Supplement S2 provides additional risk results, such as, risk maps at grid cell level (S2.1 & S2.2), at country level per month (S2.3), temporal evolution of wind and trade risks independently (S2.4), source cells and countries considered in scenario 2 (S2.5) and risk maps across scenarios (S2.6).

Appendix A. Supporting information

Supplementary data associated with this article can be found in the online version at doi:10.1016/j.prevetmed.2025.106656.

References

Aguilar-Vega, C., Bosch, J., Fernández-Carrión, E., Lucientes, J., Sánchez-Vizcaíno, J.M., 2020. Identifying spanish areas at more risk of monthly BTV transmission with a basic reproduction number approach. Viruses 12, 1158. https://doi.org/10.3390/v12101158.

AHAW, 2009. Scientific opinion on epizootic hemorrhagic disease. Efsa J. 7, 1418. https://doi.org/10.2903/j.efsa.2009.1418.

Balenghien, T., Alexander, N., Arnþórsdóttir, A.L., Bisia, M., Blackwell, A., Bødker, R., Bourquia, M., Boutsini, S., Carpenter, S., Colenutt, C., Culverwell, L., Cvetkovikj, A., Dascălu, L., Regge, N.D., Dhollander, S., Elbers, A., England, M., Filatov, S., Garros, C., Goffredo, M., Haddad, N., Høye, T.T., Hristescu, D., Khallaayoune, K., Kočišová, A., Larska, M., Lucientes, J., Mathieu, B., Miranda, M.A., Murchie, A., Nițescu, C., Ozoliņa, Z., Fonseca, I.P. da, Petrić, D., Pudar, D., Ramilo, D., Richardson, J., Seglina, Z., Sghaier, S., Stefanovska, J., Stougiou, D., Sviland, S., Tchakarova, S., Bortel, W.V., Castello, M.V., Veronesi, E., Versteirt, V., Wint, W.G.R., 2020. VectorNet data series 3: culicoides abundance distribution models for Europe and surrounding regions. Open Heal Data 7, 7. https://doi.org/10.5334/ohd.33.

Bibard, A., Martinetti, D., Giraud, A., Picado, A., Chalvet-Monfray, K., Porphyre, T., 2024a. Quantitative risk assessment for the introduction of bluetongue virus into mainland Europe by long-distance wind dispersal of culicoides spp.: a case study from sardinia. Risk Anal. https://doi.org/10.1111/risa.14345.

Bibard, A., Martinetti, D., Picado, A., Chalvet-Monfray, K., Porphyre, T., 2024b. Assessing the risk of windborne dispersal of culicoides midges in emerging epizootic hemorrhagic disease virus outbreaks in France. Transbound. Emerg. Dis. 2024. https://doi.org/10.1155/2024/5571195.

Carpenter, S., Wilson, A., Barber, J., Veronesi, E., Mellor, P., Venter, G., Gubbins, S., 2011. Temperature dependence of the extrinsic incubation period of orbiviruses in culicoides biting midges. PLoS One 6, e27987. https://doi.org/10.1371/journal.pone.0027987.

Chatellier, V., 2017. Les échanges de bovins vivants et de viande bovine dans Le Monde et dans l'UE: trajectoires productives et commerciales des principaux pays impliqués. INRA Prod. Anim. 30, 199–218. https://doi.org/10.20870/productions-animales.2017.30.3.2245.

Conte, A., Giovannini, A., Savini, L., Goffredo, M., Calistri, P., Meiswinkel, R., 2003. The effect of climate on the presence of culicoides imicola in Italy. J. Vet. Med. Ser. B 50, 139–147. https://doi.org/10.1046/j.1439-0450.2003.00632.x.

Cooley, D. googleway: Accesses Google Maps APIs to Retrieve Data and Plot Maps. R package version 2.7.8. https://CRAN.R-project.org/package=googleway.

Diego, A.C.P., Sánchez-Cordón, P.J., Sánchez-Vizcaíno, J.M., 2014. Bluetongue in Spain: from the first outbreak to 2012. Transbound. Emerg. Dis. 61, e1–e11. https://doi.org/10.1111/tbed.12068.

Dórea, F.C., Swanenburg, M., Roermund, H., Horigan, V., Vos, C., Gale, P., Lilja, T., Comin, A., Bahuon, C., Zientara, S., Young, B., Vial, F., Kosmider, R., Lindberg, A., 2017. Data collection for risk assessments on animal health (Acronym: DACRAH): final report. Efsa Support. Publ. 14, 1171E. https://doi.org/10.2903/sp.efsa.2017.en-1171.

Driessche, P. Van den, 2017. Reproduction numbers of infectious disease models. Infect. Dis. Model 2, 288–303. https://doi.org/10.1016/j.idm.2017.06.002.

Ducheyne, E., Lange, M., Stede, Y.V.Der, Meroc, E., Durand, B., Hendrickx, G., 2011. A stochastic predictive model for the natural spread of bluetongue. Prev. Vet. Med. 99, 48–59. https://doi.org/10.1016/j.prevetmed.2011.01.003.

Eagles, D., Deveson, T., Walker, P.J., Zalucki, M.P., Durr, P., 2012. Evaluation of long-distance dispersal of culicoides midges into Northern Australia using a migration model. Med. Vet. Entomol. 26, 334–340. https://doi.org/10.1111/j.1365-2915.2011.01005.x.

Eagles, D., Melville, L., Weir, R., Davis, S., Bellis, G., Zalucki, M.P., Walker, P.J., Durr, P. A., 2014. Long-distance aerial dispersal modelling of culicoidesbiting midges: case studies of incursions into Australia. Bmc Vet. Res 10, 135. https://doi.org/10.1186/1746-6148-10-135.

EC, 2023. EU agricultural outlook for markets, 2023-2035. European Commission. DG Agriculture and Rural Development, Brussels.

ESA, 2024. Bulletins hebdomadaires de veille sanitaire internationale du 31/07/2024 [WWW Document]. URL⟨https://www.plateforme-esa.fr/fr/bulletins-hebdomadaires-de-veille-sanitaire-internationale-du-31-07-2024⟩(accessed 7.24)..

ESA, 2024b. Bulletins hebdomadaires de veille sanitaire internationale du 23/01/2024 [WWW Document]. URL https://www.plateforme-esa.fr/fr/bulletins-hebdomadaires-de-veille-sanitaire-internationale-du-23-01-2024 (accessed 12.4.24).

European, C., 2024. Commission Delegated Regulation (EU) 2020/687 of 17 December 2019 supplementing Regulation (EU) 2016/429 of the European Parliament and the Council, as regards rules for the prevention and control of certain listed diseases [WWW Document]. URL⟨https://aquaculture.ec.europa.eu/knowledge-base/eu-legislation-and-relevant-international-instruments/commission-delegated-0#:~:text=Commission%20Delegated%20Regulation%20%28EU%29%202020%2F687%20of%2017%20December,the%20prevention%20and%20control%20of%20certain%20listed%20diseases⟩(accessed 8.14.24).

Gale, P., Kelly, L., Snary, E.L., 2015. Pathways for entry of livestock arboviruses into Great Britain: assessing the strength of evidence. Transbound. Emerg. Dis. 62, 115–123. https://doi.org/10.1111/tbed.12317.

García-Lastra, R., Leginagoikoa, I., Plazaola, J.M., Ocabo, B., Aduriz, G., Nunes, T., Juste, R.A., 2012. Bluetongue virus serotype 1 outbreak in the basque country (Northern Spain) 2007–2008. data support a primary vector windborne transport. PLoS One 7, e34421. https://doi.org/10.1371/journal.pone.0034421.

GDS, F., ESA, P., 2024. Description des premiers impacts sanitaires de la fièvre catarrhale ovine-sérotype 3 (FCO-3) et FCO-8 dans les troupeaux bovins et ovins français pour la saison virale 2024.

Gilbert, M., Nicolas, G., Cinardi, G., Boeckel, T.P.V., Vanwambeke, S.O., Wint, G.R.W., Robinson, T.P., 2018. Global distribution data for cattle, buffaloes, horses, sheep, goats, pigs, chickens and ducks in 2010. Sci. Data 5, 180227. https://doi.org/10.1038/sdata.2018.227.

Gondard, M., Postic, L., Garin, E., Turpaud, M., Vorimore, F., Ngwa-Mbot, D., Tran, M.-L., Hoffmann, B., 6, C.W., Savini, G., Lorusso, A., Marcacci, M., Felten, A., Roux, A.L., Blanchard, Y., Zientara, S., Vitour, D., Sailleau, C., Bréard, E., 2024. Exceptional bluetongue virus (BTV) and epizootic hemorrhagic disease virus (EHDV) circulation in France in 2023. Virus Res. 350. https://doi.org/10.1016/j.virusres.2024.199489.

Guis, H., Caminade, C., Calvete, C., Morse, A.P., Tran, A., Baylis, M., 2012. Modelling the effects of past and future climate on the risk of bluetongue emergence in Europe. J. R. Soc. Interface 9, 339–350. https://doi.org/10.1098/rsif.2011.0255.

Hartnett, E., Adkin, A., Seaman, M., Cooper, J., Watson, E., Coburn, H., England, T., Marooney, Christopher, Marooney, Christophen, Cox, A., Wooldridge, Marion, Wooldridge, Mavion, 2007. A quantitative assessment of the risks from illegally imported meat contaminated with foot and mouth disease virus to Great Britain. Risk Anal. 27, 187–202. https://doi.org/10.1111/j.1539-6924.2006.00869.x.

Hoar, B.R., Carpenter, T.E., Singer, R.S., Gardner, I.A., 2004. Probability of introduction of exotic strains of bluetongue virus into the US and into california through importation of infected cattle. Prev. Vet. Med. 66, 79–91. https://doi.org/10.1016/j.prevetmed.2004.08.006.

Karger, D.N., Schmatz, D.R., Dettling, G., Zimmermann, N.E., 2020. High-resolution monthly precipitation and temperature time series from 2006 to 2100. Sci. Data 7, 248. https://doi.org/10.1038/s41597-020-00587-y.

Kundlacz, C., Caignard, G., Sailleau, C., Viarouge, C., Postic, L., Vitour, D., Zientara, S., Breard, E., 2019. Bluetongue virus in France: an illustration of the european and Mediterranean context since the 2000s. Viruses 11, 672. https://doi.org/10.3390/v11070672.

Loeb, J., 2024. BTV-12 found in Dutch livestock. Vet. Rec. 195. https://doi.org/10.1002/vetr.4862, 360–360.

Lorusso, A., Cappai, S., Loi, F., Pinna, L., Ruiu, A., Puggioni, G., Guercio, A., Purpari, G., Vicari, D., Sghaier, S., Zientara, S., Spedicato, M., Hammami, S., Hassine, T.B., Portanti, O., Breard, E., Sailleu, C., Ancora, M., Sabatino, D.D., Morelli, D., Calistri, P., Savini, G., 2022. First detection of epizootic haemorrhagic disease virus in the european union, Italy-2022. Biorxiv 2022. https://doi.org/10.1101/2022.11.23.517495, 11.23.517495.

MASA, 2024. Maladie hémorragique épizootique (MHE): l'Etat, mobilisé pour protéger le cheptel français et ralentir la progression de la maladie, lance la campagne de vaccination Ministère de l'Agriculture, de la Souveraineté alimentaire et de la Forêt [WWW Document]. URL https://agriculture.gouv.fr/maladie-hemorragique-epizootique-mhe-letat-mobilise-pour-proteger-le-cheptel-francais-et-ralentir (accessed 10.9.24).

Massot, A., Negre, F., Vinci, C., 2021. Patterns of livestock transport in the EU and to third countries. Res. ANIT Comm. https://doi.org/10.2861/422268.

Molitorisová, A., Burke, C., 2023. Farm to fork strategy: animal welfare, EU trade policy, and public participation. Appl. Econ. Perspect. Polic. 45, 881–910. https://doi.org/10.1002/aepp.13326.

More, S., Bicout, D., Bøtner, A., Butterworth, A., Calistri, P., Koeijer, A.D., Depner, K., Edwards, S., Garin-Bastuji, B., Good, M., Schmidt, C.G., Michel, V., Miranda, M.A., Nielsen, S.S., Raj, M., Sihvonen, L., Spoolder, H., Thulke, H., Velarde, A., Willeberg, P., Winckler, C., Bau, A., Beltran-Beck, B., Carnesecchi, E., Casier, P., Czwienczek, E., Dhollander, S., Georgiadis, M., Gogin, A., Pasinato, L., Richardson, J., Riolo, F., Rossi, G., Watts, M., Lima, E., Stegeman, J.A., 2017. Vector-borne diseases. Efsa J. 15, e04793. https://doi.org/10.2903/j.efsa.2017.4793.

Mullens, B.A., Gerry, A.C., Lysyk, T.J., Schmidtmann, E.T., 2004. Environmental effects on vector competence and virogenesis of bluetongue virus in culicoides: interpreting laboratory data in a field context. Vet. Ital. 40, 160–166.

Napp, S., Garcia-Bocanegra, I., Pagès, N., Allepuz, A., ALBA, A., Casal, J., 2013. Assessment of the risk of a bluetongue outbreak in Europe caused by culicoides midges introduced through intracontinental transport and trade networks. Med. Vet. Entomol. 27, 19–28. https://doi.org/10.1111/j.1365-2915.2012.01016.x.

Rossi, R., 2020. Transport of live animals. Rep. Eur. Parliam. Res. Serv. https://www.europarl.europa.eu/RegData/etudes/ATAG/2020/646170/EPRS_ATA(2020)646170_EN.pdf.

Samset, B.H., Zhou, C., Fuglestvedt, J.S., Lund, M.T., Marotzke, J., Zelinka, M.D., 2023. Steady global surface warming from 1973 to 2022 but increased warming rate after 1990. Commun. Earth Environ. 4, 400. https://doi.org/10.1038/s43247-023-01061-4.

Santman-Berends, I.M.G.A., Brink, K.M.J.A., Van, den, Dijkstra, E., Schaik, G. van, Spierenburg, M.A.H., Brom, R., Van, den, 2024. The impact of the bluetongue serotype 3 outbreak on sheep and goat mortality in the Netherlands in 2023. Prev. Vet. Med. 231, 106289. https://doi.org/10.1016/j.prevetmed.2024.106289.

Santman-Berends, I.M.G.A., Stegeman, J.A., Vellema, P., Schaik, G.Van, 2013. Estimation of the reproduction ratio (R0) of bluetongue based on serological field data and comparison with other BTV transmission models. Prev. Vet. Med 108, 276–284. https://doi.org/10.1016/j.prevetmed.2012.11.004.

Santos, M.A.S., Gonzales, J.R., Swanenburg, M., Vidal, G., Evans, D., Horigan, V., Betts, J., Ragione, R.L., Horton, D., Dórea, F., 2023. Epizootic hemorrhagic disease (EHD) – systematic literature review report. EFSA Support. Publ. 20. https://doi.org/10.2903/sp.efsa.2023.en-8027.

Sellers, R.F., Maarouf, A.R., 1991. Possible introduction of epizootic hemorrhagic disease of deer virus (serotype 2) and bluetongue virus (serotype 11) into British Columbia in 1987 and 1988 by infected *Culicoides* carried on the wind. Can. J. Vet. Res Rev. 55, 367–370.

Simons, R.R.L., Horigan, V., Ip, S., Taylor, R.A., Crescio, M.I., Maurella, C., Mastrantonio, G., Bertolini, S., Ru, G., Cook, C., Adkin, A., 2019. A spatial risk assessment model framework for incursion of exotic animal disease into the european union member states. Micro Risk Anal. 13, 100075. https://doi.org/10.1016/j.mran.2019.05.001.

Stein, A.F., Draxler, R.R., Rolph, G.D., Stunder, B.J.B., Cohen, M.D., Ngan, F., 2015. NOAA's HYSPLIT atmospheric transport and dispersion modeling system. B Am. Meteor. Soc. 96, 2059–2077. https://doi.org/10.1175/bams-d-14-00110.1.

Team, R.C., 2022. R A Lang. Environ. Stat. Comput.. R Foundation for Statistical Computing, Vienna, Austria. https://www.R-project.org/.

Turner, J., Bowers, R.G., Baylis, M., 2013. Two-Host, Two-Vector basic reproduction ratio (R_0) for bluetongue. PLoS One 8, e53128. https://doi.org/10.1371/journal.pone.0053128.

UN, 2022. UN Comtrade | International Trade Statistics Database [WWW Document]. URL ⟨https://comtrade.un.org/?msclkid=74a9a537a9ed11ec89d3ecc170333259⟩ (accessed 3.22.22).

Versteirt, V., Balenghien, T., Tack, W., Wint, W., 2017. A first estimation of culicoides imicola and culicoides obsoletus/culicoides scoticus seasonality and abundance in Europe. Efsa Support. Publ. 14. https://doi.org/10.2903/sp.efsa.2017.en-1182.

WBVR, 2023. Bluetongue in ruminants, updates 2023 [WWW Document]. URL ⟨https://www.wur.nl/nl/onderzoek-resultaten/onderzoeksinstituten/bioveterinary-research/show-bvr/blauwtong-bij-herkauwers-updates-2023.htm⟩.

White, S.M., Sanders, C.J., Shortall, C.R., Purse, B.V., 2017. Mechanistic model for predicting the seasonal abundance of culicoides biting midges and the impacts of insecticide control. Parasite Vector 10, 162. https://doi.org/10.1186/s13071-017-2097-5.

Wittmann, E.J., Mellor, P.S., Baylis, M., 2002. Effect of temperature on the transmission of orbiviruses by the biting midge, culicoides sonorensis. Med. Vet. Entomol. 16, 147–156. https://doi.org/10.1046/j.1365-2915.2002.00357.x.

WMO, 2024. Climate change indicators reached record levels in 2023: WMO [WWW Document]. URL https://public.wmo.int/news/media-centre/climate-change-indicators-reached-record-levels-2023-wmo (Accessed 10.28.24).

WOAH, 2022. Terrestrial Code Online Access - WOAH - World Organisation for Animal Health [WWW Document]. URL https://www.woah.org/en/what-we-do/standards/codes-and-manuals/terrestrial-code-online-access/ (Accessed 10.14.22).

WOAH, 2023. WAHIS: World Animal Health Information System [WWW Document]. URL https://wahis.woah.org/#/home.

Zientara, S., Sailleau, C., Dujardin, P., Bréard, E., Vitour, D., 2024. Émergence de la maladie hémorragique épizootique en France en 2023: impacts et perspectives futures. Virologie 28, 1–2. https://doi.org/10.1684/vir.2024.1035.